Modelling and Simulation of an Underwater Acoustic Communication Channel

D. Kraus
Hochschule Bremen

Modelling and Simulation of an Underwater Acoustic Communication Channel

D. Kraus[a,b], P.P. Kalangi[a]

[a]University of Applied Sciences Bremen, Neustadtswall 30, 28199 Bremen, Germany,
e-mail: krausd@fbe.hs-bremen.de
[b]ATLAS ELEKTRONIK GmbH, Sebaldsbrücker Heerstr. 235, 28305 Bremen, Germany

Summary

Underwater acoustic communication is a rapidly growing field of research and engineering. The wave propagation in an underwater sound channel is mainly affected by channel variations, multipath propagation, and Doppler spreading which keep a lot of hurdles for achieving high data rates and transmission robustness. Furthermore, the usable bandwidth of an underwater sound channel is typically only a few kHz at large distances. In order to achieve high data rates it is mandatory to employ bandwidth efficient modulation techniques. Thus, we present a reliable simulation environment for underwater acoustic communication applications that models the sound channel by incorporating multipath propagation, surface and bottom reflection coefficients, attenuation, spreading and scattering losses as well as the transmitter/receiver device employing Quadrature-Phase-Shift-Keying modulation. To demonstrate the quality of the simulation tool a simulation result is presented.

1. Introduction

The application of underwater communication, which once were exclusively military, are extending into commercial fields such as remote control in off-shore oil industry, pollution monitoring in environmental systems, collection of scientific data recorded at ocean-bottom stations, speech transmission between divers, and mapping of the ocean floor, as well as for the discovery of new resources.

The possibility of data transmission without a physical connection enables gathering of data from submerged instruments without human intervention and unobstructed operation of unmanned or autonomous underwater vehicles (UUVs, AUVs). An untethered underwater communication can be only established by an acoustical link.

However, underwater acoustic wave propagation mainly gets affected by

- **Channel Variations,**
  i.e. variations in temperature, salinity and pH value, hydrostatic pressure and surface/bottom roughness.
- **Multipath Propagation**
  The channel can be considered as a wave guide and due to the reflections at surface and bottom we have the consequence of multipath propagation.
- **Attenuation**
  Acoustic energy is partly transformed into heat and lost due to sound scattering by inhomogeneities.
- **Doppler Spreading**
  Transmitter and receiver movements as well as wave propagations including reflections at moving ocean surfaces cause Doppler spreading in the received signal.

Channel variations, multipath propagation and Doppler spreading keep a lot of hurdles for the achievement of high data rates and robust communication links. Moreover, the increasing absorption towards higher frequencies limits the usable bandwidth typically to only a few kHz at large distances. Therefore, to achieve high data rates bandwidth efficient modulation techniques have to be employed.

In this paper a reliable simulation environment for underwater acoustic communication applications (reducing the need of sea trails) is presented. It models the sound channel by incorporating multipath propagation, surface and bottom reflection coefficients, attenuation, spreading and scattering losses as well as the transmitter/receiver devices employing Quadrature Phase-Shift Keying (QPSK) modulation techniques. Furthermore to express the quality of the simulation tool a simulation result is presented for an exemplary scene.

2. Sound Propagation Modelling

2.1 Homogenous Waveguide, Image Method

For underwater acoustic communication the simplest waveguide model, i.e. a range-independent, isovelocity water column with infinitely extended boundaries, as shown in Fig. 1 is considered.

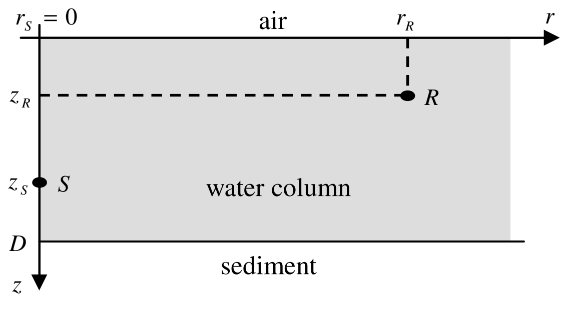

Figure 1: Homogenous ocean waveguide model.

The field produced by a point source at $(0, z_S)$ in the absence of boundaries is given by

$$P(r,z,\omega) = A\frac{e^{ikR}}{R}, \quad k = \frac{\omega}{c}.$$

Now, to satisfy the boundary conditions at the surface and bottom of the waveguide we have to add additional sources by applying the image method.

The image method superimposes the free-field solution with the fields produced by image sources. In the wave guide case, sound will be multiply reflected between the two boundaries, requiring an infinite number of image sources to be included, cf. [1, 2].

Fig. 3 shows a schematic representation of the contributions from the physical source at depth z_S and the first three image sources.

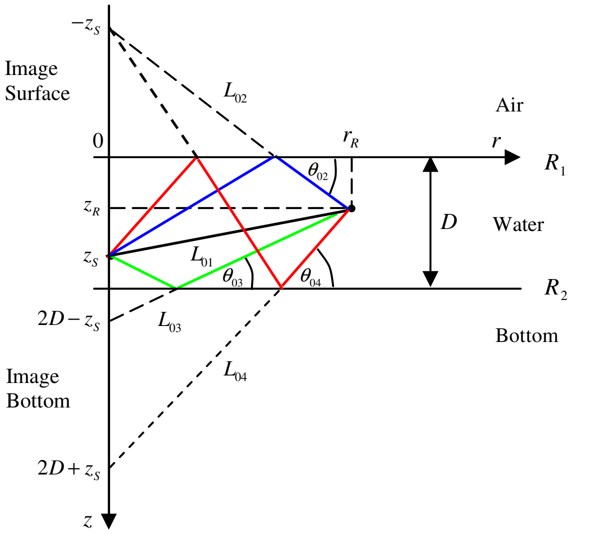

Figure 3: Homogenous ocean waveguide model.

Successive continuation of the image source technique leads to the ray expansion of the total field which can be written in the form

$$\begin{aligned} P(r,z,\omega) = A(\omega)\sum_{m=0}^{\infty}\Bigg(& R_1^m(\theta_{m1},\omega)R_2^m(\theta_{m1},\omega)\frac{\exp(-i\,kL_{m1})}{L_{m1}} \\ & + R_1^{m+1}(\theta_{m2},\omega)R_2^m(\theta_{m2},\omega)\frac{\exp(-i\,kL_{m2})}{L_{m2}} \\ & + R_1^m(\theta_{m3},\omega)R_2^{m+1}(\theta_{m3},\omega)\frac{\exp(-i\,kL_{m3})}{L_{m3}} \\ & + R_1^{m+1}(\theta_{m4},\omega)R_2^{m+1}(\theta_{m4},\omega)\frac{\exp(-i\,kL_{m4})}{L_{m4}}\Bigg) \end{aligned}$$

with
$$\begin{aligned} L_{m1} &= \sqrt{r_R^2 + (2Dm - z_s + z_R)^2} \\ L_{m2} &= \sqrt{r_R^2 + (2Dm + z_s + z_R)^2} \\ L_{m3} &= \sqrt{r_R^2 + (2D(m+1) - z_s - z_R)^2} \\ L_{m4} &= \sqrt{r_R^2 + (2D(m+1) + z_s - z_R)^2} \end{aligned}$$

and
$$\begin{aligned} \theta_{m1} &= \arctan([2Dm - z_S + z_R]/r_R) \\ \theta_{m2} &= \arctan([2Dm + z_S + z_R]/r_R) \\ \theta_{m3} &= \arctan([2D(m+1) - z_S - z_R]/r_R) \\ \theta_{m4} &= \arctan([2D(m+1) + z_S - z_R]/r_R). \end{aligned}$$

2.2 Reflection and Scattering

The reflection and transmission geometry of a plane wave incident on a plane interface separating two loosy homogeneous fluid media is depicted in Fig. 4.

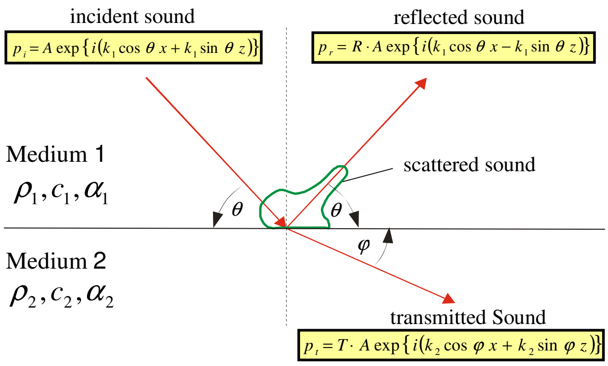

Figure 4: Reflection and transmission at a plane fluid-fluid interface.

Exploiting the boundary conditions, i.e. the continuity of pressure and vertical particle velocity, the complex reflection coefficient can be determined by

$$R'(\theta,\omega) = \frac{m\sin\theta - \sqrt{n^2 - \cos^2\theta}}{m\sin\theta + \sqrt{n^2 - \cos^2\theta}}$$

with

$$m = \frac{\rho_2}{\rho_1}, \quad n = \frac{k_2}{k_1} = \frac{k_{2,R} + ik_{2,I}}{k_{1,R} + ik_{1,I}}, \quad k_{i,R} = \frac{\omega}{c_i}, \quad k_{i,I} = \alpha_i.$$

The parameter ρ_i, c_i and α_i denote the density, sound velocity and attenuation of the ith medium, respectively.

The magnitude and argument of the complex reflection coefficient versus grazing angle is shown for typical bottom types in Fig. 5.

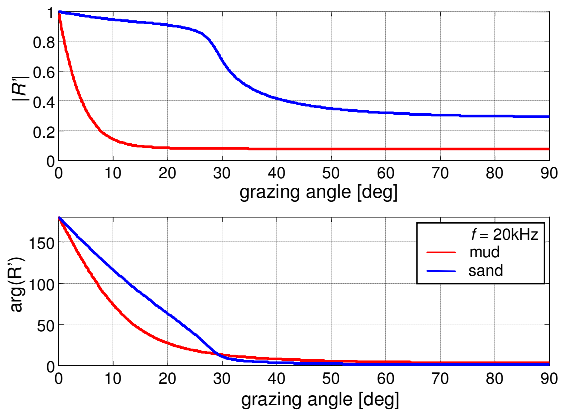

Figure 5: Magnitude and argument of the complex reflection coefficient.

Rough boundaries (surface, bottom) cause additional attenuation of the mean acoustic field propagating in the ocean waveguide. The effect of scattering from rough boundaries is thought to be simply an additional loss to the specularly reflected (coherent) component resulting from the scattering of energy away from the specular direction, cf. Fig. 4. If the ocean bottom or surface can be modelled as randomly rough surface, and if the roughness is small compared to the acoustic wavelength, the reflection loss due to the scattering process can be incorporated by modifying the reflection coefficient as follows.

$$R(\theta,\omega) = R'(\theta,\omega)\exp\left(-\Gamma^2/2\right), \quad \Gamma = 2k\sigma\cos\theta$$

where σ denotes the root mean square roughness given as a function of wind speed or grain size for surface and bottom roughness respectively, cf. [1, 2, 3].

2.3 Sound Attenuation

The acoustic energy of sound waves propagating in the ocean is partly absorbed, i.e. energy is transformed into heat, and lost due to sound scattering by inhomogeneities. The frequency dependent attenuation of sound can be satisfactory accurate determined using the Francois/Garrison formula, cf. [2, 3]. Representative attenuation curves, parameterized by salinity, water temperature and pH-value, are shown in Fig. 6.

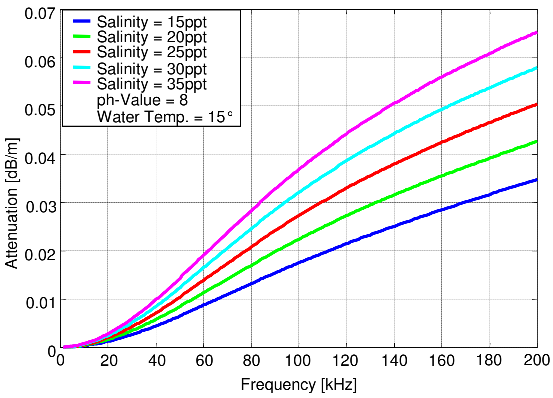

Figure 6: Attenuation of sound

2.4 Ambient noise

The received underwater acoustic communication signals are imbedded in the ambient noise of the ocean. The ambient noise is mainly composed by vessel noise (own and traffic), biological noise, thermal noise and sea state dependent noise. The vessel and biological noise levels have to be set in accordance with the own platform properties, traffic situation and current biological life. The thermal and the sea state noise are calculated exploiting Knudsen or Wentz curves, cf. [2, 3]. A typical ambient noise spectrum is depicted in Fig. 7.

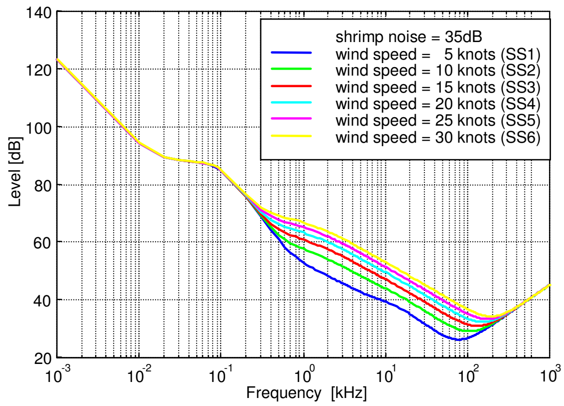

Figure 7: Ambient noise spectrum

3. Simulation Result

The underwater acoustic simulation concept, including the modulation and demodulation units for transmit and receive, is depicted in Fig. 8. For a first demonstration of the abilities of the underwater acoustic channel model it suffices to show the time delays and transmission losses of a transmitted pulse that is travelling over various ray paths towards the receiver, which is exemplarily shown for the first 8 ray paths in Fig. 9.

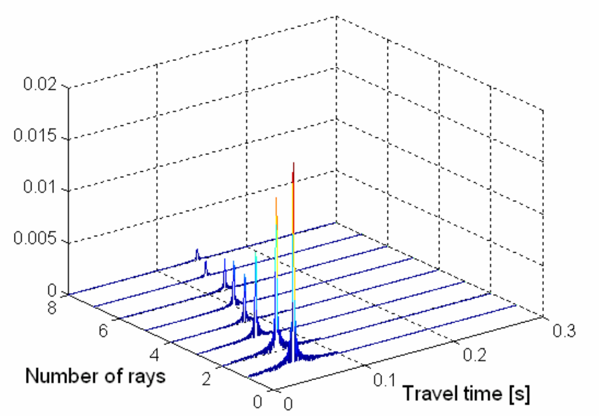

Figure 9: Multipath propagation indicating time delays and transmission losses.

References

[1] L.M. Brekhovskikh, Y.P. Lysanov: Fundamentals of Ocean Acoustics, Springer, 1998.

[2] F.B. Jensen et al.: Computational Ocean Acoustics, Springer, 2000.

[3] H. Medwin, C.S. Clay:, Fundamentals of Acoustical Oceanography, Academic Press, 1998.

[4] J.G. Proakis: Digital Communications, McGraw-Hill, 2001.

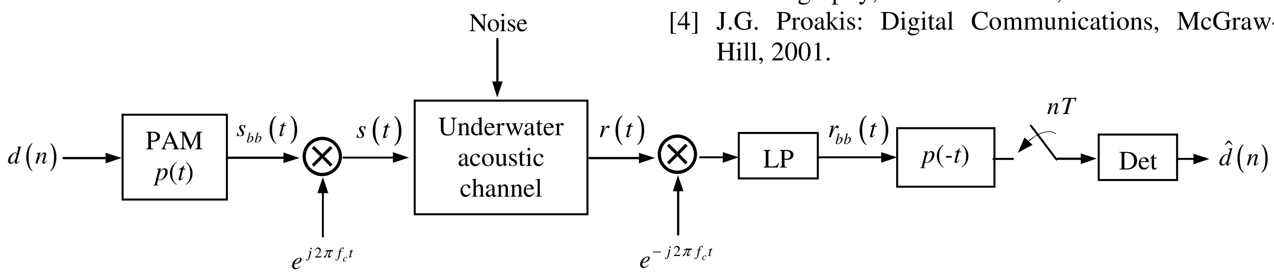

Figure 8: Underwater acoustic simulation scheme.